Surface acoustic wave driven light modulation

Mike van der Poel (1), Markus Beck (2), Maria B. Dühring (3), Maurício M. de Lima (4), Lars H. Frandsen (1), Christophe Peucheret (1), Ole Sigmund (3), Uwe Jahn (2), Jørn M. Hvam (1), and Paulo Santos (2)
1) COM-DTU, NanoDTU, Technical University of Denmark, DK-2800 Kgs. Lyngby, Denmark 2) Paul-Drude Institut für Festkörperfysik, D-10117 Berlin, Germany, 3) Department of Mechanical Engineering, NanoDTU, Technical University of Denmark, DK-2800 Kgs. Lyngby, Denmark, 4) Material Science Institute, University of Valencia, 46071 Valencia, Spain

Abstract: *Si and GaAs Mach-Zehnder type light modulators with surface acoustic wave (SAW) excitation are demonstrated. Relative modulation depths of 40% at 950 nm and 5% at 1550 nm in the GaAs and Si samples respectively are achieved at SAW frequency around 600 MHz. Active area dimensions are down to 20 x 20 μm.*

Introduction

Compact, integrated light modulation devices are essential components in many photonic applications and have received large attention in recent years [1-4]. Of particular interest is the realization of modulation functionality in the Si material system [3-5] as this has the potential for seamless integration with electronics.

An important class of light modulators work by achieving uneven phase shifting of the light in the two arms of a Mazh-Zehnder interferometer (MZI). The change in relative phase and resulting constructive or destructive interference of the light waves at the exit port is the mechanism behind the light modulation. The principle of the phase change can be based upon shifting of the modal index of the guided wave by utilizing e.g. the thermo-optic [2], the electro-optical effect [3] or the Kerr effect [4].

In this paper we present light modulation in compact Si and GaAs [1] MZI devices with phase shifting resulting from surface acoustic wave (SAW) modulation of the waveguides.

SAW modulator

A SAW consists of a strain field propagating along the surface of a solid. The field strength decays towards the bulk with the wavelength as the characteristic decay length. The SAW field can be excited by applying an electrical RF field to an interdigital transducer (IDT) on a piezo electric material. The SAW strain field results in a periodic refractive index modulation $\Delta n \sin(\omega_{SAW} t)$ in the material, where ω_{SAW} is the SAW angular frequency. This is the primary

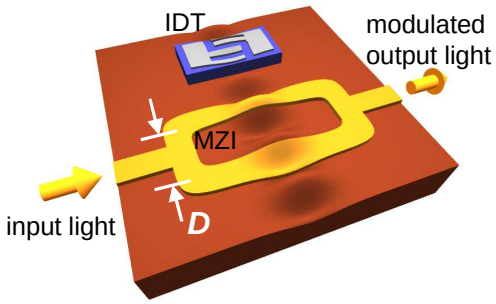

Fig. 1: Schematic representation of an MZI device with SAW modulation. Separation of the MZI arms, *D*, is an odd number of half SAW wavelenghts, so that tbhe SAW field modulates the two arms in opposite phase.

mechanism behind the optical phase change $\Delta\phi_1$ and $\Delta\phi_2$ in arm 1 and 2 of a SAW based MZI modulator respectively. For an interaction length L, the light waves of common angular frequency ω in arm 1 and 2 of the MZI undergo a harmonic phase shift of magnitude $\Delta\phi_{1,2} = \omega\Delta n_{1,2}L/c$, where c is the speed of light in vacuum. The index change is proportional to the strength of the SAW strain field and thus changes sign during a SAW cycle. We note that it follows from this, that the induced phase shift is proportional to the square root of the SAW power.

In the experiments reported here, we use a SAW propagating perpendicularly to a MZI with arm spacing D corresponding to an odd number of half SAW waves (fig. 1). In this configuration, the SAW results in a modal index variation of opposite phase in the two arms thus increasing the phase difference of the two light waves when combined at the exit port of the MZI device. Besides the acoustic phase moulation, the light field at the exit port also dependends on the static phase difference $\Delta\phi_s$ between the two interferometer arms. A path-length difference in the two arms of Δx results in a static phase difference $\Delta\phi_s = \omega n\Delta x/c$, where n is the modal index of the guided light. We write the electrical field E_{out} of the light at the exit port as

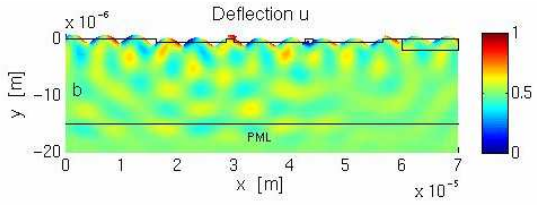

Fig. 2: SAW propagating in the MZI from the left to the right. The colorbar indicates the deflections in the x-direction.

$$E_{out} = \frac{E_0}{2}\{\sin[\omega t - \Delta\phi_1 \sin(\omega_{SAW} t)] + \sin[\omega t - \Delta\phi_2 \sin(\omega_{SAW} t - \pi/2) - \Delta\phi_s]\}, \quad (1)$$

where E_0 is the electrical field amplitude at the MZI input.

The light modulation in a MZI device as described above [1] depends strongly on the static phase difference between the two interferometer arms. For a small amplitude of the phase modulation $\Delta\phi_{1,2}$, for instance, the maximum modulation at the SAW frequency is achieved with a static phase difference $\Delta\phi_s = \pi/2$, while $\Delta\phi_s = 0$ or π results in no modulation at the SAW frequency and instead a modulation at twice the SAW frequency.

SAW modelling

To understand and improve the interaction of the SAW elastic field with the optical field in the waveguides a numerical model of the MZI is made. The SAW generation by IDTs is modeled using a 2D finite-element model of a piezoelectric, inhomogeneous material implemented in the high-level programming language 'Comsol Multiphysics'. To prevent unwanted reflections of the SAW from the boundaries of the calculation domain perfectly matched layers [6] are employed to absorb the elastic and electric field at the sides and at the bottom of the domain. The solution of this model gives the stresses in the material introduced by the SAW, from which the associated change in refractive index in the two wave guides can be calculated. This model is successively coupled to an optical model where the time independent wave equation is solved as an eigenvalue problem giving the effective refractive index of the fundamental mode in the waveguides.

With this numerical model the propagation of the SAW in the MZI can be studied. In fig. 2, a SAW is generated at the left part of the surface and propagating in the right direction through a GaAs MZI. It is observed that a part of the SAW propagates through the MZI and another part is redirected into the bulk substrate because of the disturbance at the surface caused by the wave guides. Figure 3 shows the

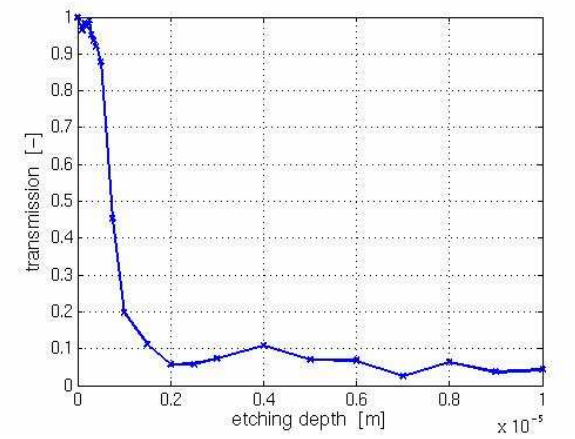

Fig. 3: The transmission of the SAW as function of the etching depth.

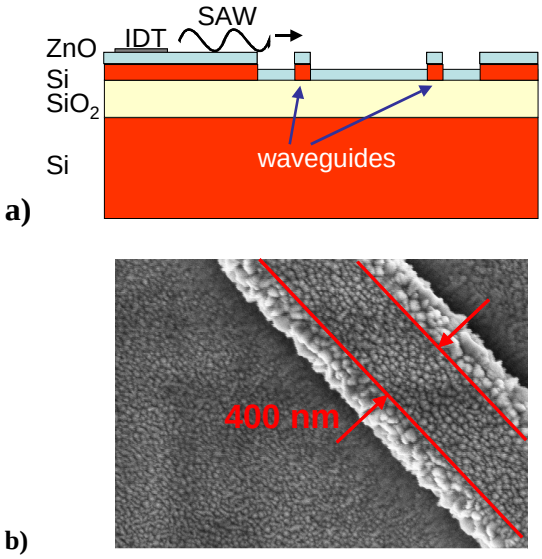

Fig. 4: a) Schematic edge view of SOI wafer with waveguides. b) SEM micrograph with top view of 400 nm ridge waveguide covered with ZnO.

transmission of the SAW (calculated as the part of the deflections in the x-direction that reaches the marked rectangle in the right corner of the domain in fig. 1) as function of the etching depth. It is seen that for small etching depths almost the entire SAW is transmitted, but for larger depths most of the SAW energy will be reflected back or disappear into the bulk substrate.

This model can be used to simulate the acousto-optical interaction in the MZI from the experiments and by a parameter study of the geometry it can be determined how the geometry should be changed in order to improve the optical modulation.

Devices

Devices based upon the Si and GaAs material system have been fabricated.

The GaAs MZI devices were fabricated on a (Al,Ga)As waveguide structure grown by molecular beam epitaxy on a GaAs (100) wafer. The waveguide core consists of a 300-nm-thick GaAs core grown on a 1500-nm-thick $Al_{0.2}Ga_{0.8}As$ cladding layer. The acoustic waves were generated by a split-finger IDT with an aperture of 120 µm and operating at an acoustic wavelength λ_{SAW}=5.6 µm. The waveguides were fabricated by combining contact optical lithography with plasma etching. Further details of the fabrication process can be found in Ref. [1].

The Si based samples were made on a Si-on-insulator (SOI) wafer with a top 340 nm thick Si layer. 400 nm wide single-mode ridge waveguides were defined by electron-beam lithography (fig. 4a). Si itself is not a piezo electrical material: for the electric SAW excitation, the sample is covered with a 500 nm layer of piezoelectric ZnO before IDT deposition. Scanning electron microscopy (SEM) of the sample after ZnO deposition (fig. 4b) shows a corrugated surface with ZnO crystallites grown from all surfaces. This is ex-

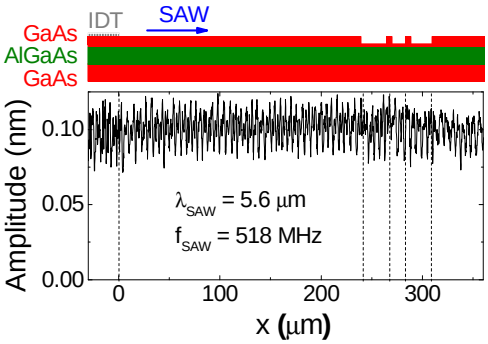

Fig. 5: Transmission of a SAW across the GaAs MZI structure.

pected to lead to the undesirable effect of increased 1) optical waveguide losses and 2) scattering of the SAW wave at Si etch steps. The former is discussed in a section below. To investigate the latter, we perform interferometric measurements of sample surface displacement. Fig. 5 shows interferometric measurements of the amplitude of the acoustic wave normal to the surface in similar structures on a GaAs/AlGaAs sample. Consistent with the calculations discussed above, the reflections of the wave at the grooves and ridges of the structure are small. In the SOI structures, we observe considerably stronger reflections.

Modulation experiments

The optical properties of the GaAs MZI devices were measured by coupling light to the cleaved edge of the waveguides using a tapered fiber and collecting the transmitted light using a microscope objective. As a light source, we used a CW superluminescence diode with peak emission at 950 nm and full width of half maximum of approx. 50 nm. The transmitted intensity was detected with a time resolution of 300 ps using a Si avalanche photodiode. Fig. 6 compares the time dependence of the transmitted intensity (normal-

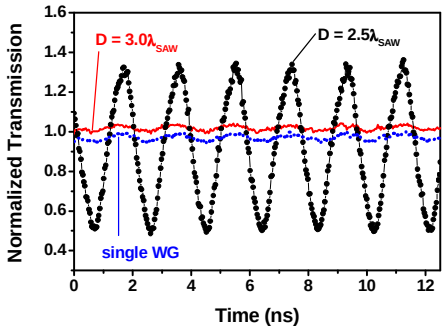

Fig. 6: Transmission of MZI devices with waveguide separation D = 3 λ_{SAW} (solid line) and 2.5 λ_{SAW} (dots). The dotted line shows the transmission in a control structure where the MZI arms have been replaced by a single waveguide. All measurements were carried out by coupling an RF-power P_{IDT}=60 mW to the IDTs.

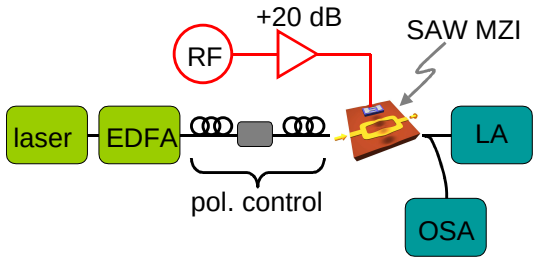

Fig.7: Experimental setup for characterizing SOI modulator.

ized to the transmission in the absence of acoustic excitation) of devices with distances *D* between the MZI arms of 3 λ_{SAW} (solid line) and 2.5 λ_{SAW} (dots). All measurements were carried out by coupling an rf-power P_{IDT}=60 mW to the IDTs. For the devices with 3 λ_{SAW}, as well as in control structures where the MZI arms have been replaced by a single waveguide (dotted line in fig. 6), the relative modulation does not exceed 2 %. In devices with D = 2.5 $\lambda_{SAW,}$ where the MZI arms are excited with opposite acoustic phases, the relative modulation reaches 40 %. These results demonstrate the large modulation performance achieved by the simultaneous out-of-phase modulation of the MZI arms. By employing focusing IDTs, we were able to further increase the performance and to reduce the length of the MZI arms down to approx. 15 µm. [1].

The experimental setup of the modulation experiments carried out on the SOI devices can be summarized as follows (fig. 7): A fiber-coupled, tunable CW laser and Er doped fiber amplifier (EDFA) was used as light source in the wavelength range 1530-1580 nm. A polarization controller was used to achieve transverse-electric (TE) polarized light before using a tapered fiber to couple the light into the MZI device under test. Modulation properties of the light output from the MZI were then analyzed using a lightwave analyzer (LA).

The MZI were deliberately made with a path length difference in the two interferometer arms of 34 µm so as to have a wavelength-dependent static phase

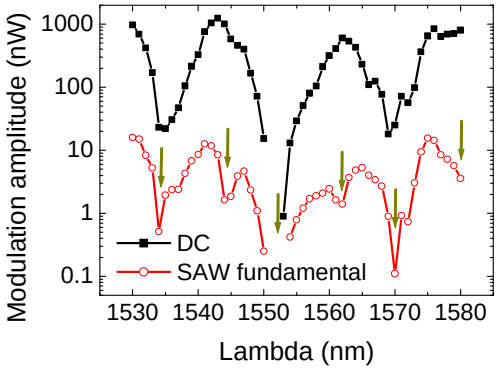

Fig. 8: Transmission (black line, filled symbols) and modulation (red line, open symbols) spectrum of SOI MZI with arm separation of *D*=4.5λ_{SAW}. RF power to IDTs P_{RF}= 50 mW.

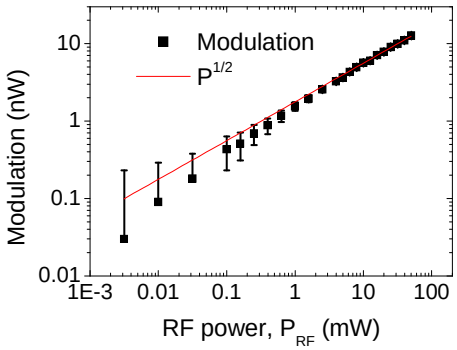

Fig. 9: Modulationamplitude at SAW frequency vs. RF power to the IDT, P_{RF}.

$\Delta\phi_s = \omega n \Delta x/c$ as mentioned above. This results in a sinusoidally varying DC transmission spectrum of the device (fig. 8). The overall transmission of the device at constructive interference at the exit port was about –20 dB. This poor performance is primarily ascribed to the two T-splitters in the MZI. These topology-optimized ridge-waveguide splitters [7] were designed without ZnO coverage in mind. We also believe that the deviations from a sinusoidal transmission spectrum are due to the T-splitters.

The MZI had an arm separation of D=4.5λ_{SAW} corresponding to an out-of-phase phase-change in the two interferometer arms when SAW modulation is applied to the device. It follows from eq. 1 that the modulation spectrum at the SAW frequency will display minima at both the DC transmission maxima and minima in agreement with fig. 8 (minima marked with arrows). Furthermore it is concluded from eq. 1, that the observed modulation at the SAW fundamental frequency is consistent with a refractive change of 2.3×10^{-5}. This value is also consistent with the absence of measurable higher harmonics in the modulated light at all wavelengths. The relative modulation in the investigated wavelength range varied from 0% to 8%. Finally, we mention that the modulation amplitude vs. RF power was measured, and a reasonable agreement with the expected $P_{SAW}^{1/2}$ dependency, as demonstrated in fig. 9.

Conclusion

SAW-driven MZI is a promising technology for compact light modulators in integrated semiconductor platforms such as Si and GaAs.

Acknowledgments

This project is supported by the EU network of excellence ePIXnet. Mike van der Poel acknowledges support from the Danish Research Council.

References

1 M. M. de Lima, Jr., M. Beck, R. Hey, and P. V. Santos, Appl. Phys. Lett., vol. 89, p. 121104, 2006.
2 E. A. Camargo, H. M. H. Chong, and R. M. De La Rue, Opt. Express, vol. 12, p. 588, 2004.
3 R. S. Jacobsen et al., Nature, vol. 44, p. 199, 2006.
4 M. Hochberg et al., Nature Mater., vol. 5, p. 703, 2006.
5 M. Lipson, J. Lightwave Techn., vol. 23, p. 4222, 2005.
6 U. Basu and A. K. Chopra,, Comput. Methods Appl. Mech. Engrg., vol. 192, p. 1337 (2003).
7 L. H. Frandsen, paper CMV4, Conference of Lasers and Electro-Optics (CLEO), 2006.